Journal of Photochemistry and Photobiology A: Chemistry 214 (2010) 152–160

Contents lists available at ScienceDirect

Journal of Photochemistry and Photobiology A: Chemistry

journal homepage: www.elsevier.com/locate/jphotochem

# A study on the NIR-luminescence emitted from ternary lanthanide [Er(III), Nd(III) and Yb(III)] complexes containing fluorinated-ligand and 4,5-diazafluoren-9-one

Song Dang[a,b], Jiang-Bo Yu[a], Xiao-Fei Wang[a,b], Zhi-Yong Guo[a], Li-Ning Sun[a], Rui-Ping Deng[a], Jing Feng[a], Wei-Qiang Fan[a,b], Hong-Jie Zhang[a,*]

[a] State Key Laboratory of Rare Earth Chemistry and Physics, Changchun Institute of Applied Chemistry, Chinese Academy of Sciences, Changchun 130022, PR China
[b] Graduate School of the Chinese Academy of Sciences, Beijing, PR China

ARTICLE INFO

*Article history:*
Received 24 March 2010
Received in revised form 26 May 2010
Accepted 16 June 2010
Available online 23 June 2010

*Keywords:*
Ternary lanthanide
Fluorinated-ligand
NIR-luminescence
Antenna effect

ABSTRACT

A series of lanthanide complexes Ln(tfnb)$_3$dafone, Ln(hfth)$_3$dafone and Ln(pfnd)$_3$dafone (Ln = Er, Nd and Yb) with fluorinated-ligand 1-(2-naphthyl)-4,4,4-trifluoro-1,3-butanedionate (Htfnb), 4,4,5,5,6,6,6-heptafluoro-1-(2-thienyl)hexane-1,3-dione (Hhfth) and 4,4,5,5,6,6,7,7,8,8,9,9,10,10,10-pentadecafluoro-1-(naphthalen-2-yl)decane-1,3-dione (Hpfnd) served as main sensitizers, respectively, and 4,5-diazafluoren-9-one (dafone) as the synergistic ligand were synthesized. Upon excitation at the maximum absorption of the ligands, the complexes all show the characteristic near-infrared (NIR) luminescence of the corresponding $Ln^{3+}$ ions, which is due to efficient energy transfer from the ligands to the central $Ln^{3+}$ ions *via* an antenna effect. Moreover, an indirect excitation model is proposed and the influence of ligands on the luminescence properties of the complexes is further discussed.

Crown Copyright © 2010 Published by Elsevier B.V. All rights reserved.

## 1. Introduction

Ligand-sensitized, near-infrared (NIR) luminescent lanthanide(III) complexes are of considerable importance due to their unique photophysical properties [1], especially their application in optical amplifiers (such as Er-based emission) [2,3], in laser systems (such as Nd-based emission) [4], and in fluoroimmunoassays (such as Yb-based emission) [5]. One challenge in this field is to design of sensitizing ligands which can provide effective intramolecular energy transfer from the coordinated ligands to the central lanthanide ions, *via* an "antenna effect". Since Weissman first reported the light-emission characteristic of a lanthanide β-diketone complex in 1942 [6], numerous lanthanide complexes with β-diketone ligands have been studied in detail due to their excellent luminescence properties.

Another beneficial effect of the organic ligands is to prevent water from binding the first coordination sphere that may quench the luminescence efficiently [7–9]. Furthermore, the replacement of C–H bonds with lower-energy C–F oscillators in the β-diketone ligand is able to lower the vibration energy of the ligand, which decreases the energy loss caused by ligand vibration and enhances the emission intensity of the lanthanide ion [10,11]. Therefore, fluorination of hydrogen-containing ligands, together with exclusion of coordinated water of the lanthanide complex, can increase the lifetime of NIR-luminescence of the lanthanide complex [12].

Herein, in order to provide a further understanding of the effect of aromatic C–F substitution of the ligand on the photophysical properties of Er(III), Nd(III) and Yb(III) complexes, the ligands, 1-(2-naphthyl)-4,4,4-trifluoro-1,3-butanedionate (Htfnb), 4,4,5,5,6,6,6-heptafluoro-1-(2-thienyl)hexane-1,3-dione (Hhfth) and 4,4,5,5,6,6,7,7,8,8,9,9,10,10,10-pentadecafluoro-1-(naphthalen-2-yl)decane-1,3-dione (Hpfnd) are served as primary sensitizers for complexes Ln(tfnb)$_3$dafone (abbreviated as Ln**1**), Ln(hfth)$_3$dafone (abbreviated as Ln**2**) and Ln(pfnd)$_3$dafone (abbreviated as Ln**3**), in which the ligand 4,5-diazafluoren-9-one (dafone) acts as the synergistic ligand (Ln = Er, Nd and Yb). The complexes were characterized by Fourier Transform Infrared (FT-IR) spectra, diffuse reflectance (DR) and photoluminescence spectroscopy. In addition, an indirect excitation model is proposed and the antenna effect of the lanthanide complexes is discussed in detail.

## 2. Experimental

### 2.1. Materials and characterization

Erbium oxide ($Er_2O_3$, 99.99%), neodymium oxide ($Nd_2O_3$, 99.99%) ytterbium oxide ($Yb_2O_3$, 99.99%) and gadolinium

* Corresponding author. Tel.: +86 431 85262127; fax: +86 431 85698041.
*E-mail address:* hongjie@ciac.jl.cn (H.-J. Zhang).

1010-6030/$ – see front matter. Crown Copyright © 2010 Published by Elsevier B.V. All rights reserved.
doi:10.1016/j.jphotochem.2010.06.019

oxide ($Gd_2O_3$, 99.99%) were purchased from Yue Long Chemical Plant (Shanghai, China). Sodium metal (≥98%, A.R.) and 1,10-phenanthroline monohydrate (phen·$H_2O$, 99%, A.R.) were bought from Beijing Fine Chemical Co. (Beijing, China). 1-(2-naphthyl)-4,4,4-trifluoro-1,3-butanedionate (Htfnb), 4,4,5,5,6,6,6-heptafluoro-1-(2-thienyl)hexane-1,3-dione (Hhfth), and 2′-acetonaphthone (98%) were purchased from Acros Organics Co. (Geel, Belgium), and pentadecylfluoropropionate (98%) was from Aldrich. All these reagents were used directly without further purification.

The CHN elemental analyses were carried out on a VarioEL analyzer. The NMR spectra were recorded on a Bruker DRX 400 spectrometer. FT-IR spectra were measured within a 4000–400 $cm^{-1}$ region on an American BIO-RAD Company model FTS135 infrared spectrophotometer with the KBr pellet technique. DR measurements were recorded at room temperature at a SHIMADZU UV-3600 spectrophotometer. The fluorescence spectra were measured on a Horiba Jobin Yvon Fluorolog-3 fluorescence spectrophotometer, equipped with a 450 W Xe-lamp as the excitation source and a monochromator iHR320 equipped with a liquid-nitrogen-cooled R5509-72 PMT as detector. The time-resolved measurements, were done by using the third harmonic (355 nm) of a Spectra-physics Nd:YAG laser with a 5 ns pulse width and 5 mJ of energy per pulse as the source, and the NIR-emission lines were dispersed by a HORIBA Jobin Yvon emission monochromator iHR320 equipped with liquid-nitrogen-cooled R5509-72 PMT, and the data were analyzed with a LeCroy WaveRunner 6100 1 GHz Oscilloscope. The luminescence lifetime was calculated by Origin 8.0 software package. The low-temperature phosphorescence spectrum of the $Gd(pfnd)_3(H_2O)_2$ complex was measured on a Hitachi F-4500 spectrophotometer at liquid-nitrogen temperature (77 K).

### 2.2. Synthesis of the ligand dafone

Ligand dafone was synthesized according to the procedure described in the reference [13]. 1,10-phenanthroline (16 g, 88 mmol) and potassium hydroxide (16 g, 288 mmol) were dissolved in 1000 mL water. Potassium permanganate (40 g, 256 mmol) was added in 600 mL water and heated to dissolve and then added slowly into the hot solution mentioned above. After completing the addition, the solution was refluxed for 3 h and filtered hot. The cool filtrate was extracted with chloroform and dried over anhydrous $MgSO_4$. The crude product was purified by recrystallization from dichloromethane to give 4,5-diazafluoren-9-one (6.8 g, 43% yield) as yellow-colored needles. Anal. Calcd. for $C_{11}H_6N_2O$: C, 72.52%; H 3.32%; N, 15.38%; O, 8.78%. Found: C, 72.31%; H 3.40%; N, 15.42%; O, 8.69%. $^1H$ NMR ($CDCl_3$, 400 MHz) $\delta$ 7.33, (2H, q), 7.96 (2H, q), 8.77 (2H, q). GC–MS: 182.

### 2.3. Synthesis of the ligand Hpfnd

Ligand Hpfnd was synthesized according to the procedure described in the reference [14] with a minor modification. The modified method of a typical Claisen condensation procedure was used as follows. Metal sodium thread (0.345 g, 15 mmol) was added into dry anhydrous ethanol (30 mL). The reaction mixture was stirred for 15 min at room temperature, after which 2′-acetonaphthone (1.720 g, 10 mmol) and pentadecylfluoropropionate (5.560 g, 10 mmol) were added. The mixture was then stirred for 48 h at room temperature. The resulting mixture was acidified to pH 2-3 by using hydrochloric acid (2 M solution). The white precipitate was collected and dried at 50 °C under vacuum for 4 h (4.11 g, 71% yield based on 2′-acetonaphthone). Anal. Calcd. for $C_{16}H_9F_7O_2$: C, 42.42%; H, 1.60%. Found: C, 42.50%; H, 1.48%. $^1H$ NMR (DMSO, 400 MHz) $\delta$ 7.16, (1H, s), 7.65 (1H, td), 7.71 (1H, td), 8.03 (1H, d), 8.06-8.11 (2H, m), 8.15 (1H, d), 8.87 (1H, s), 12.38 (1H, broad).

### 2.4. Synthesis of complexes Ln**1** to Ln**3**

The $LnCl_3$ (Ln = Er, Nd, Yb and Gd) ethanol solution was prepared by dissolving the corresponding $Ln_2O_3$ in concentrated hydrochloric acid (HCl). The products were dissolved with anhydrous ethanol. The concentration of the $Ln^{3+}$ (Ln = Er, Nd, Yb and Gd) ions was determined by titration with a standard ethylenediaminetetraacetic acid (EDTA) aqueous solution.

In the typical synthesis, Ln**1** (Ln = Er, Nd and Yb) was prepared as follows: 3 mmol Htfnb and 1 mmol dafone were dissolved in anhydrous ethanol at room temperature, then 1 M sodium hydroxide solution was added dropwise to the solution to adjust the pH to neutral. 1 mmol $LnCl_3$ in ethanol solution was then added to the mixture under stirring. The mixture was heated to reflux for 6 h. The precipitates were collected after filtration and dried at 70 °C under vacuum overnight. Yield: 65% (based on $Ln^{3+}$ ion). The syntheses of complexes Ln**2** and Ln**3** were similar to that of Ln**1**, except Hhfth or Hpfnd were used instead of Htfnb, respectively. The complexes were recrystallized from ethanol.

*Elemental analysis*: For Er**1**, Calcd.: C, 55.45%; H, 2.88%; N, 2.44%. Found: C, 55.61%; H, 2.47%; N, 2.75%. For Nd**1**, Calcd.: C, 56.58%; H, 2.94%; N, 2.49%. Found: C, 56.89%; H, 2.58%; N, 2.30%. For Yb**1**, Calcd.: C, 55.16%; H, 2.86%; N, 2.43%. Found: C, 55.50%; H, 2.64%; N, 2.21%. For Er**2**, Calcd.: C, 37.41%; H, 1.60%; N, 2.13%. Found: C, 37.67%; H, 1.85%; N, 2.37%. For Nd**2**, Calcd.: C, 38.08%; H, 1.63%; N, 2.17%. Found: C, 38.27%; H, 2.34%; N, 2.34%. For Yb**2** Calcd.: C, 37.24%; H, 1.59%; N, 2.12%. Found: C, 37.47%; H, 1.71%; N, 2.32%. For Er**3**, Calcd.: C, 41.62%; H, 1.61%; N, 1.37%. Found: C, 41.80%; H, 1.84%; N, 1.54%. For Nd**3**, Calcd.: C, 42.09%; H, 1.63%; N, 1.38%. Found: C, 42.29%; H, 1.87%; N, 1.62%. For Yb**3**, Calcd.: C, 41.50%; H, 1.61%; N, 1.36%. Found: C, 41.76%; H, 1.85%; N, 1.59%.

### 2.5. Synthesis of $Gd(pfnd)_3(H_2O)_2$ complex

0.9 mmol of Hpfnd was dissolved in anhydrous ethanol at room temperature, and 0.3 mmol $GdCl_3$ ethanol solution was then added to the mixture under stirring. The mixture was heated to reflux for 6 h. The white powder was filtered and washed with ethanol. The product was dried at 60 °C under vacuum overnight. For $Gd(pfnd)_3(H_2O)_2$, Calcd.: C, 38.08%; H, 1.64%; N, 1.48%. Found: C, 38.27%; H, 1.87%; N, 1.34%.

## 3. Results and discussion

### 3.1. FT-IR and DR spectra

The chemical structure of the complexes Ln**1** to Ln**3** is outlined in Scheme 1. The FT-IR spectra of the Er**1** to Er**3**, as shown in Fig. 1, would be discussed as examples of the complexes. For all the Er-complexes, bands appearing in the range of 400–438 $cm^{-1}$ correspond to $\nu_{Er\text{-}O}$ vibrations and the peak at 515 $cm^{-1}$ can be observed, which should assigned to a $\nu_{Er\text{-}N}$ vibration. It offers evidence the coordination bonds were formed between erbium and dafone, and erbium and tfnb, hfth, and pfnd, respectively [15]. Strong carbon–fluorine bands appear from 1000 to 1300 $cm^{-1}$ [16].

The DR spectra of Er**1**, Er**2** and Er**3** are shown in Fig. 2(left), of Nd**1**, Nd**2** and Nd**3** are shown in Fig. 3(left), and of Yb**1**, Yb**2** and Yb**3** are shown in Fig. 4 (left), respectively. The spectra all exhibit broad absorption bands in the range from 200 to 400 nm, which could correspond to electronic transitions from the ground-state level ($\pi$) $S_0$ to the excited level ($\pi^*$) $S_1$ of the organic ligands [17]. In the region above 400 nm in these figures, each absorption band corresponds

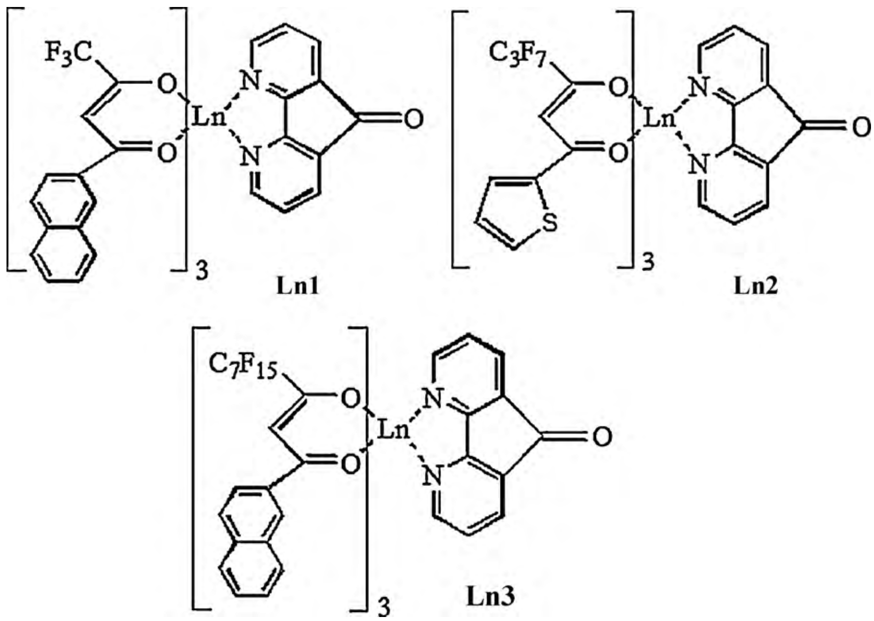


**Scheme 1.** Chemical structures of Ln**1**, Ln**2** and Ln**3**.

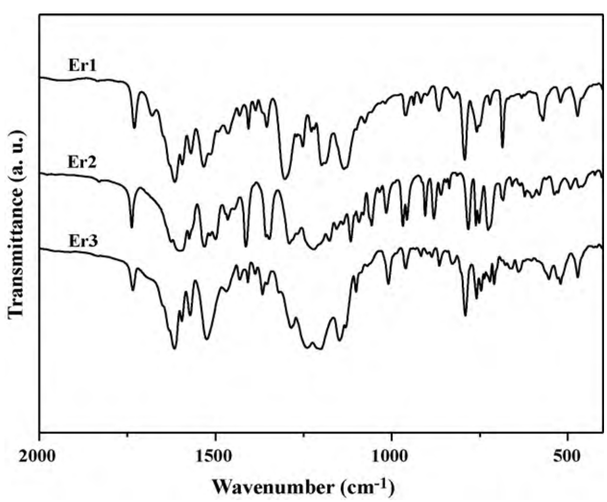


**Fig. 1.** The FT-IR spectra of Er**1**, Er**2** and Er**3**.

to the characteristic transition between two spin-orbit coupling levels of the lanthanide ion (see the right pictures of Figs. 2–4, respectively). Based on the energy level scheme of each ion, these bands can be assigned to the transitions from the ground levels $^4I_{15/2}$, $^4I_{9/2}$ and $^2F_{7/2}$ to the higher energy levels for the Er, Nd and Yb-complexes, respectively [18,19].

### 3.2. Antenna effects

Lanthanide β-diketone complexes exhibit intense emissions when UV irradiation, due to the effective intramolecular energy transfer from the coordinating ligands to the central lanthanide ions, which in turn undergo the corresponding radiative emitting process, called "antenna effect". It exhibits in spectrum as the overlaps between the excitation spectrum of resulting complex and the absorption spectra of the corresponding ligands [20,21]. The Er**1**, Er**2** and Er**3** complexes will be taken as examples to discuss the antenna effect. The excitation spectrum of the Er**1** complex (monitored at 1540 nm) and the absorption spectra of ligands (tfnb and dafone) are shown in Fig. 6 (A). The overlaps between the exci-

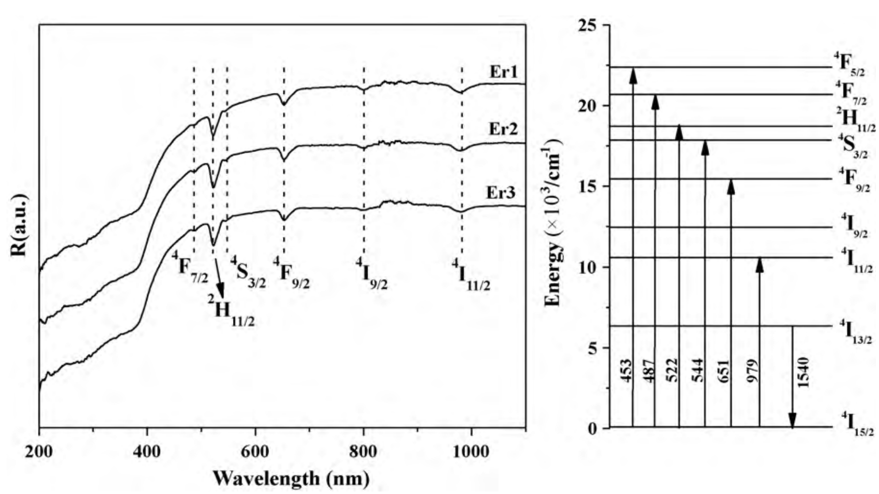


**Fig. 2.** The DR spectra of Er**1**, Er**2** and Er**3** (left). The energy level diagrams of $Er^{3+}$ ion (right). The transitions of the bands (nm) are shown by using arrows.

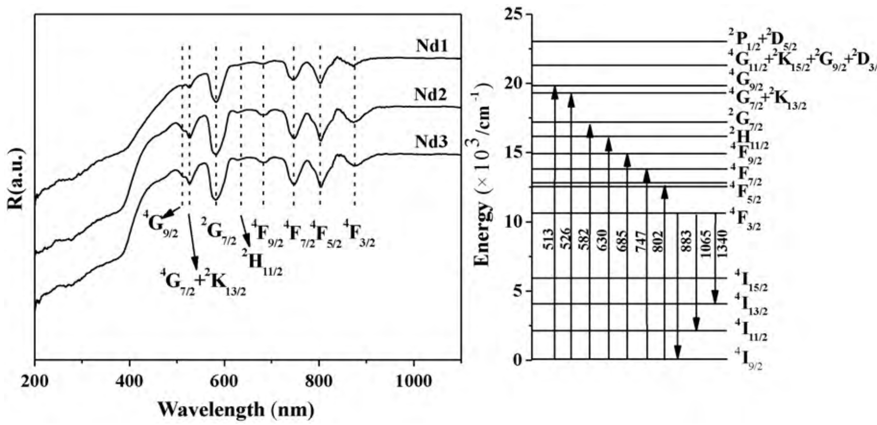


**Fig. 3.** The DR spectra of Nd**1**, Nd**2** and Nd**3** (left). The energy level diagrams of $Nd^{3+}$ ion (right). The transitions of the bands (nm) are shown by using arrows.

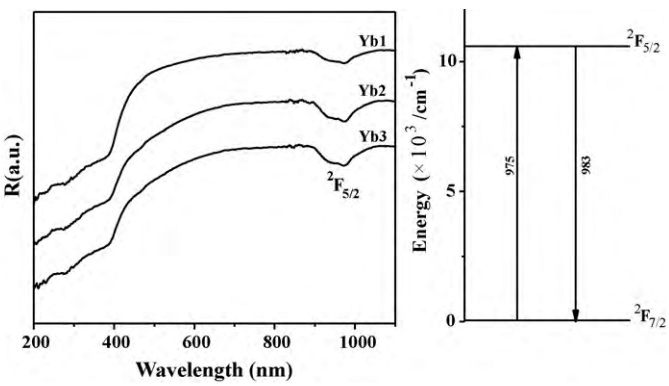


**Fig. 4.** The DR spectra of Yb**1**, Yb**2** and Yb**3** (left). The energy level diagrams of $Yb^{3+}$ ion (Right). The transitions of the bands (nm) are shown by using arrows.

tation band of Er**1** and the absorption bands of ligands (tfnb and dafone) can been observed clearly, which indicates that central $Er^{3+}$ ion in Er**1** complex can be efficiently sensitized by the ligands (tfnb and dafone), an antenna effect [22–24]. Additionally, Förster model [25,26], which considers the overlap between the emission spectrum of the donor and the absorption spectrum of the acceptor, is essential to energy transfer phenomenon. It is observed from Fig. 5(B) that there are overlaps between the absorption spectrum of $ErCl_3$ in ethanol and the emission spectra of ligands (tfnb and dafone), which suggests that both tfnb and dafone ligands can sensitize the luminescence of the central $Er^{3+}$ ion [27,28]. Meanwhile, it is also worth noting that the overlap between the excitation spectrum of Er**1** complex and the absorption spectrum of tfnb ligand is much larger than that between the excitation spectrum of Er**1** complex and the absorption spectrum of dafone ligand, which suggests that the antenna effect of tfnb is more efficient than that of dafone for the central $Er^{3+}$ ion. Consequently, we come to the conclusion that the intramolecular energy transfer in Er**1** complex mainly occurs between tfnb ligand and the central $Er^{3+}$ ion [29].

It is suggested from Fig. 6 (or Fig. 7) that the central $Er^{3+}$ ion in the Er**2** (or Er3) complex can be sensitized by both hfth (or pfnd) and dafone ligands through an antenna effect, and hfth (or pfnd) are a more efficient sensitizer than dafone for the luminescence of the central $Er^{3+}$ ion. Comparison with Fig. 5 (or Fig. 7), in Fig. 6 it is interesting to notice that the overlap between the hfth ligand and the Er**2** complex is larger than that between the tfnb (or pfnd) ligand and the corresponding complex Er**1** (or Er**3**), which may imply the antenna effect of hfth ligand on the central $Er^{3+}$ is more efficient than those of ligands tfnb and pfnd. And a better intramolecular energy transfer from the hfth ligand to the central $Er^{3+}$ ion in the Er-complex can be expected. Considering the area of the overlaps between ligand and its corresponding complex being an important factor for the luminescence intensity of the complex, it can be predicted that the hfth ligand can sensitize the $Er^{3+}$ ion more efficiently in comparison with tfnb (or pfnd) ligand, and the Er**2** complex containing hfth ligand may have the strongest luminescence intensity, while the Er**3** complex with pfnd ligand have the second stronger intensity and the luminescence of the Er**1** complex with tfnb ligand is the weakest [29].

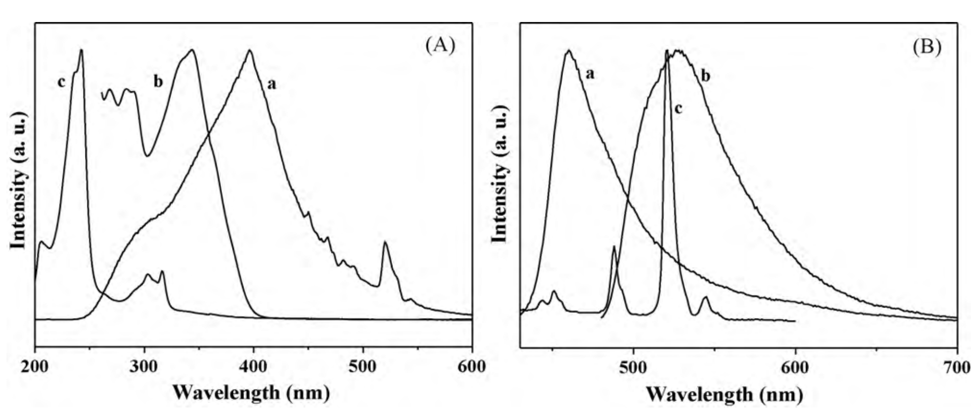


**Fig. 5.** (A) The excitation spectrum for Er**1** as solid state (a, monitored at 1540 nm), absorption spectra of tfnb (b) and dafone (c) at $5 \times 10^{-4}$ M in ethanol. (B) Emission spectra of tfnb (a, excited at 395 nm) and dafone (b, excited at 452 nm) at $5 \times 10^{-4}$ M in ethanol. Absorption spectrum of $ErCl_3$ at $5 \times 10^{-4}$ M in ethanol (c). All spectra are normalized to a constant intensity at the maximum.

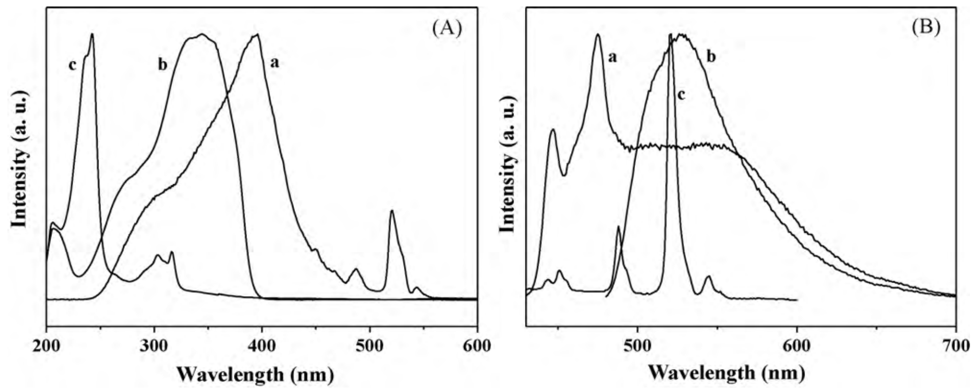


**Fig. 6.** (A) The excitation spectrum for Er**2** as solid state (a, monitored at 1539 nm), absorption spectra of hfth (b) and dafone (c) at 5 × $10^{-4}$ M in ethanol. (B) Emission spectra of hfth (a, excited at 416 nm) and dafone (b, excited at 452 nm) at 5 × $10^{-4}$ M in ethanol. Absorption spectrum of $ErCl_3$ at 5 × $10^{-4}$ M in ethanol (c). All spectra are normalized to a constant intensity at the maximum.

### *3.3. Luminescence properties*

In the excitation spectra of Er**1**, Er**2** and Er**3** complexes (Fig. S1), broad bands ranging from 260 to 505 nm are observed, which can be assigned to the absorption of the organic ligands alongside with some excitation bands originating from the characteristic absorption transitions of the $Er^{3+}$ ion. These f–f transitions can be assigned to $^4I_{15/2} \rightarrow {}^4F_{5/2}$ (451 nm), $^4I_{15/2} \rightarrow {}^4F_{7/2}$ (488 nm), $^4I_{15/2} \rightarrow {}^2H_{11/2}$ (521 nm) and $^4I_{15/2} \rightarrow {}^4S_{3/2}$ (545 nm) of the $Er^{3+}$ ion. It is worth noting that these absorption transitions are weaker than those of the ligands, which proves that luminescence sensitization *via* excitation the ligands is much more efficient than direct excitation of the $Er^{3+}$ ion. Similarly, Fig. S2 exhibits the excitation spectra of three Nd-complexes, broad bands ranging from 240 to 555 nm are observed which is assigned to the absorption of the ligands. It is also observed some small bands arising from f–f absorption transitions of the $Nd^{3+}$ ion in the excitation bands. The bands correspond to $^4I_{9/2} \rightarrow {}^4G_{9/2}$ (513 nm), $^4I_{9/2} \rightarrow {}^4G_{7/2} + {}^2K_{13/2}$ (526 nm) and $^4I_{9/2} \rightarrow {}^2G_{7/2}$ (581 nm) of the $Nd^{3+}$ ion. These absorption transitions are weaker than those of the ligands, which confirms that luminescence sensitization by excitation the ligands is much more efficient than the direct excitation of the $Nd^{3+}$ ion. The excitation spectra of Yb**1**, Yb**2** and Yb**3** were obtained by monitoring the characteristic emission of the $Yb^{3+}$ ion at 983 nm (Fig. S3). The excitation spectra are dominated by a broad band ranging from 240 to 550 nm for three complexes, which due to the absorption of the organic ligands and are in agreement with those in the DR spectra (Fig. 4).

The NIR-emission spectra of Er**1**, Er**2** and Er**3** complexes were obtained upon excitation of the ligands ($\lambda_{ex}$ = 395 nm), as shown in Fig. 8. In the three curves, the emission bands cover large spectra ranges extending from 1450 to 1635 nm, with the emission maximal all located at 1540 nm. The obtained emissions are attributed to the typical $^4I_{13/2} \rightarrow {}^4I_{15/2}$ transition of the $Er^{3+}$ ion. The Er-complexes are particularly interesting for application in amplification since the transition around 1540 nm is in the right position for the third telecommunication window [30,31]. It is also noticed that there is a little difference among the emission intensities of the Er-complexes containing different fluorinated ligands (tfnb, hfth and pfnd), which indicates ligands may have some influences on the luminescence intensity of the complexes [32,33]. The Er**2** complex containing hfth ligand has the strongest luminescence intensity and the broadest band, which may be attributed to the most efficient intramolecular energy transfer from hfth ligand to the central $Er^{3+}$ ion, followed with the Er**3** complex with pfnd ligand, and the Er**1** complex with tfnb ligand has the weakest intensity. This phenomenon is in agreement with the discussion in the part of antenna effect, as shown in Figs. 5–7.

Upon excitation of the ligand absorption band at 395 nm, characteristic NIR-luminescence of the $Nd^{3+}$ ion was obtained for Nd**1**, Nd**2** and Nd**3** complexes (shown in Fig. 9). The emission spectra of the Nd-complexes consists three bands around 884 nm, 1065 nm, and 1340 nm, corresponding to the f–f transitions $^4F_{3/2} \rightarrow {}^4I_{9/2}$, $^4F_{3/2} \rightarrow {}^4I_{11/2}$ and $^4F_{3/2} \rightarrow {}^4I_{13/2}$, respectively. The strongest emission is observed around 1065 nm, while the emissions at 884 and 1340 nm are weaker. The profiles of the emission bands and the

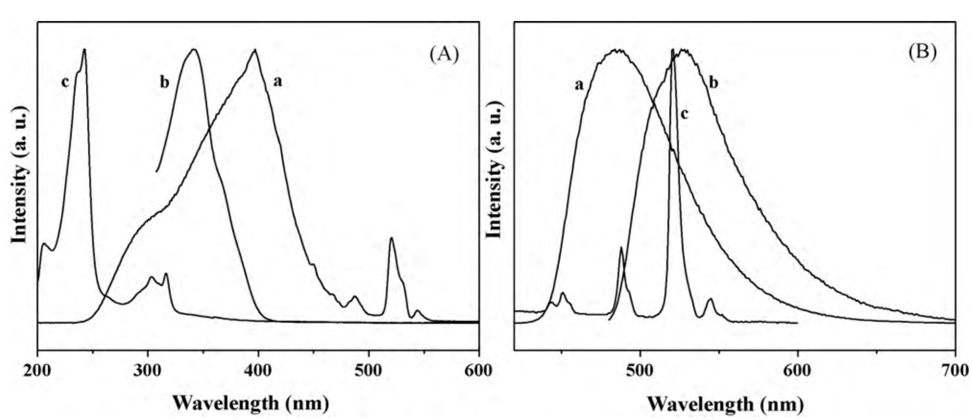


**Fig. 7.** (A) The excitation spectrum for Er**3** as solid state (a, monitored at 1540 nm), absorption spectra of pfnd (b) and dafone (c) at 5 × $10^{-4}$ M in ethanol. (B) Emission spectra of pfnd (a, excited at 394 nm) and dafone (b, excited at 452 nm) at 5 × $10^{-4}$ M in ethanol. Absorption spectrum of $ErCl_3$ at 5 × $10^{-4}$ M in ethanol (c). All spectra are normalized to a constant intensity at the maximum.

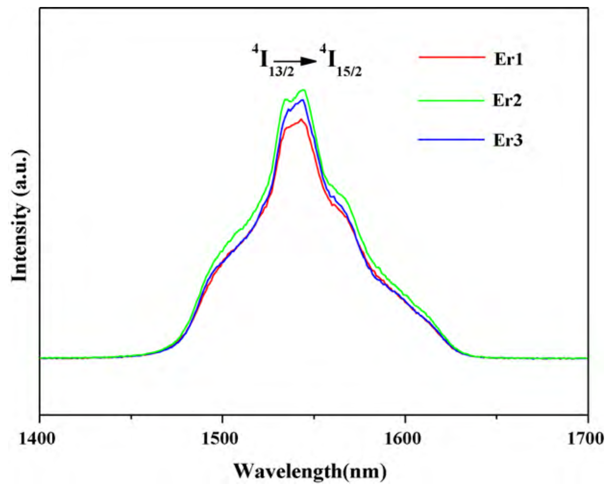


**Fig. 8.** Emission spectra of Er**1**, Er**2** and Er**3** complexes ($\lambda_{ex}$ = 395 nm).

relative intensity of the $Nd^{3+}$ luminescence for the Nd-complexes are in agreement with previously reported spectra of organic Nd-complexes [34,35]. The strongest emission around 1065 nm is potentially applied to the laser system, while the emission band at 1340 nm offers the opportunity to develop new materials suitable for optical amplifier operating at 1.3 μm [36,37].

Fig. 10 displays the emission spectra of the Yb complexes by exciting at 395 nm. The emission spectra all show the characteristic emission bands for $Yb^{3+}$ ion at 983 nm, which are assigned to the $^2F_{5/2} \to {}^2F_{7/2}$ transition. It is clearly shown that the emissions are not a single sharp band but a covering of bands ranging from 910 to 1130 nm arising at lower and higher energies [38]. Similar splitting has been reported previously [30,39], which can be attributed to the splitting of the emitting levels as a consequence of ligand-field effects [27]. The simple f–f energy level structure of the $Yb^{3+}$ ion made it important in laser emission, since there is no excited-state absorption on reducing the effective laser cross-section, no up-conversion, no concentration quenching and no absorption in the visible range. The intense $Yb^{3+}$ ion absorption lines are well suitable for laser diode pumping in this range and the smaller stokes shift (about 650 $cm^{-1}$) between absorption and emission reduces the thermal loading of the materials during laser operation [40]. Moreover, $Yb^{3+}$ emission occurs in the NIR region (around 1000 nm) where biological tissues and fluids (e.g. blood) are relatively transparent, and development of $Yb^{3+}$ complexes for various analytical and chemosensor applications is really promising, such as probe for fluoroimmuno-assays and in vivo applications [41,42].

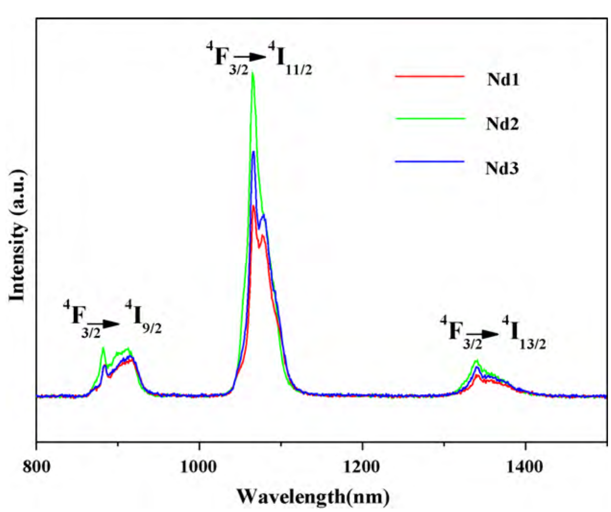


**Fig. 9.** Emission spectra of Nd**1**, Nd**2** and Nd**3** complexes ($\lambda_{ex}$ = 395 nm).

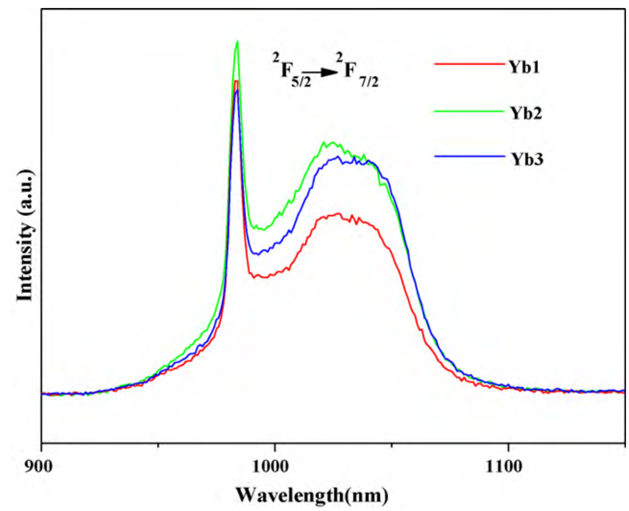


**Fig. 10.** Emission spectra of Yb**1**, Yb**2** and Yb**3** complexes ($\lambda_{ex}$ = 395 nm).

Upon excitation at 395 nm and monitored around the most intense emission lines (at 1540 nm for $Er^{3+}$ ion, at 1065 nm for the $Nd^{3+}$ ion and at 983 nm for the $Yb^{3+}$ ion, respectively), the luminescence lifetimes have been recorded in order to explore the coordination environment around the lanthanide ions in these complexes. The results fit well with monoexponential decays (Table 1), indicating that a unique and consistent coordination environment is present around the lanthanide ions [25]. It is clear that the lifetimes of the Ln**2** complexes with the hfth ligand are the longest ones, followed with those of the Ln**3** complexes containing the pfnd ligand, and the Ln**1** complexes of the tfnb ligand have the shortest lifetimes (Ln = Er, Nd and Yb). It is reasonable to deduce that the hfth ligand can transfer the energy most efficiently to the central ions in the corresponding complexes, which is in good agreement with antenna effect mentioned above.

### 3.4. Intramolecular energy transfer

Direct excitation is demanding because the lanthanide ions are characterized by very low absorption coefficient due to the strictly parity forbidden of f–f transitions in the lanthanide ions. It has to form lanthanide complexes with organic ligands which strongly absorb light in the UV region and transfer the energy from the triplet states of the ligands to the resonance levels of the $4f^n$ configuration of the lanthanide ions. Due to the strong absorption within a large wavelength range, the β-diketones are one of the most popular ligands for lanthanide ions and consequently have been targeted to

**Table 1**
Luminescence lifetimes of the complexes as solid states.

| Complexes | Lifetimes (μs) | Complexes | Lifetimes (μs) | Complexes | Lifetimes (μs) |
|---|---|---|---|---|---|
| Er**1** | 2.00 | Nd**1** | 1.21 | Yb**1** | 8.77 |
| Er**2** | 2.26 | Nd**2** | 1.69 | Yb**2** | 10 |
| Er**3** | 2.08 | Nd**3** | 1.26 | Yb**3** | 10 |

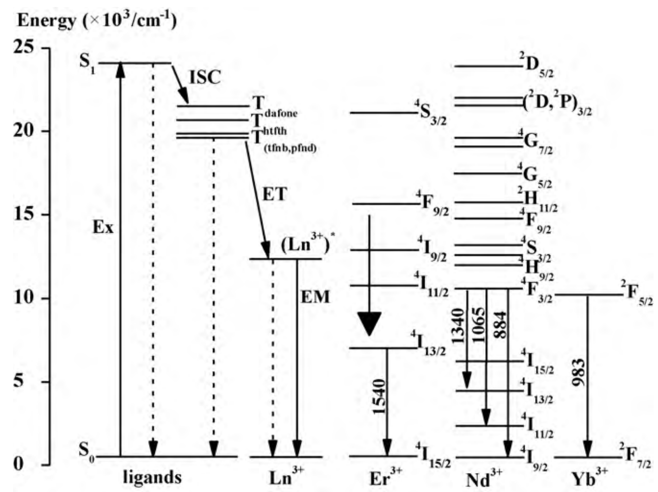


**Scheme 2.** Model for the main intramolecular energy transfer process (left) and energy diagram of the 4f levels of the $Er^{3+}$, $Nd^{3+}$ and $Yb^{3+}$ ions (right).

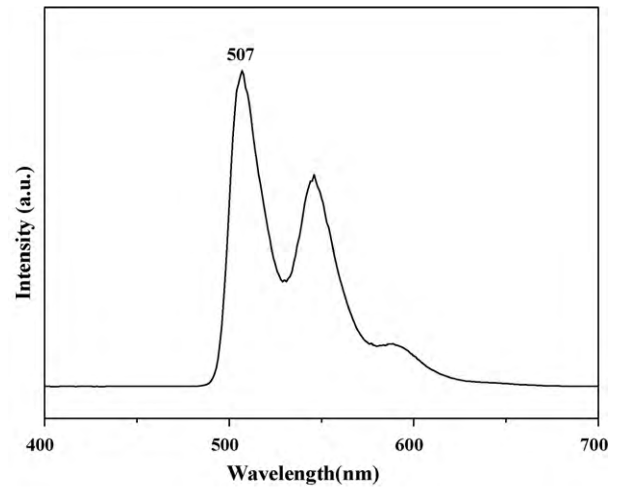


**Fig. 11.** The phosphorescence spectrum of $Gd(pfnd)_3(H_2O)_2$ complex at $5 \times 10^{-4}$ M in DMF ($\lambda_{ex}$ = 342 nm) at 77 K after a delay time of 1 s.

sensitize the lanthanide luminescence efficiently [43–47]. Moreover, the ability of the β-diketones and the lanthanide ions to form adducts is strong, and the resulting lanthanide complexes are stable enough for practical usage. In our case, the characteristic emissions of $Ln^{3+}$ ion are obtained upon excitation at the maximum absorption of organic ligands in the complexes, which indicates that the organic ligands can shield the lanthanide ions from their surroundings well and are able to transfer the absorbed energy to the central $Ln^{3+}$ ions, *via* an antenna effect. This is in agreement with the excitation results mentioned above. Therefore, a model is proposed to represent the indirect excitation process (see Scheme 2). Firstly, the ligands absorb the energy and are excited from the singlet $S_0$ ground state to the singlet $S_1$ excited state. Then the energy in the $S_1$ state is transferred to the triplet excited state of the ligands *via* the intersystem-crossing, and followed by the relaxation from the upper 4f levels to the first excited states of the $Ln^{3+}$ ions, resulting in the emission of the sensitized $Ln^{3+}$ ions.

Scheme 2 depicts a detailed scheme of the energy transfer process of the $Ln^{3+}$ (Ln = Er, Nd and Yb) ions. For the Er-complexes shown in Fig. 8, the emission bands centered at 1540 is assigned to the $^4I_{13/2} \rightarrow {}^4I_{15/2}$ transition of the $Er^{3+}$ ion. It means that through intramolecular energy transfer process the excitation energy is transferred from the ligands to the 4f levels of the $Er^{3+}$ ions, followed by the relaxation from the upper 4f levels to $^5F_5$ and $^5I_6$ first excited states of the $Er^{3+}$ ions, and then decays to $^4I_{13/2}$ with emissions of 1540 nm. The energy transfer process of the Nd-complexes is displayed in Fig. 9. The obtained band at 884, 1065 and 1340 nm can be assigned to the $^4F_{3/2} \rightarrow {}^4I_{9/2}$, $^4F_{3/2} \rightarrow {}^4I_{11/2}$ and $^4F_{3/2} \rightarrow {}^4I_{13/2}$ transitions of $Nd^{3+}$ ions, respectively. Firstly, the ligands absorb the energy and transfer it to the 4f levels of the $Nd^{3+}$ ions through an intramolecular process. Then a relaxation to $^4F_{3/2}$ level happens, followed by decay to $^4I_{9/2}$, $^4I_{11/2}$ and $^4I_{13/2}$ exhibiting emissions at 884, 1065 and 1340 nm, respectively. For the Yb-complexes, the $Yb^{3+}$ ion has the advantage for the laser emission because of its simple energy level scheme, consisting of only two levels, the $^2F_{7/2}$ ground state and the $^2F_{5/2}$ excited state. The obtained characteristic band at 983 nm is attributed to the $^2F_{5/2} \rightarrow {}^2F_{7/2}$ transition of the $Yb^{3+}$ ion (Fig. 10).

According to the Dexter's theory [48], the energy difference between the resonance level of the $Ln^{3+}$ ion and the triplet state of the ligand is crucial for efficient energy transfer. If the energy gap is too big, the overlap between the donor and the accepter will diminish, and finally the energy transfer rate constant would decrease sharply. In contrast, if the energy gap is too small, there will be an energy back-transfer from the $Ln^{3+}$ ions to the resonance levels of the triplet states of the ligands. The triplet state energy levels of tfnb and hfth is 19,700 and 20,400 $cm^{-1}$, respectively [49]. The triplet state energy level of pfnd is 19,724 $cm^{-1}$ found by examining the phosphorescence spectrum of the $Gd(pfnd)_3(H_2O)_2$ complex in DMF solution at 77 K (see Fig. 11) [50,51]. The ligands can match well with the 4f levels of the $Er^{3+}$ ion, $Nd^{3+}$ ion and the $Yb^{3+}$ ion, and obtain an efficient NIR-luminescence of the corresponding lanthanide ion. It is also known that the water molecules in the first coordination sphere of the complexes can deactivate the excited vibration manifold [52,53]. Therefore, the second ligand, dafone, was introduced in our lanthanide complexes, in order to effectively saturate the first coordination sphere of lanthanide ions and protect the central lanthanide ions against the water molecules that may quench the luminescence. Also, the second ligands can absorb excitation energy and transfer the energy to the excited states of the central ions. The combination of both ligands has essentially complementary absorption spectra in the UV region and effectively sensitizes over a wide wavelength range followed by transferring the energy to the central $Ln^{3+}$ ions.

It is believed that, to some extent, the differences in the ligand structure have influence on the luminescence behavior of the corresponding complexes. It was reported that longer fluorinated alkyl chains produce a shell effect due to the larger steric bulk of the bigger ligands [54], resulting a more suppression of the quenching effects, such as O–H, to the luminescence of the complex. In our case, three β-diketones including tfnb, hfth, and pfnd with different functional groups were selected to synthesize the desired complexes. The emission intensity sequence of these complexes is *I* (Ln**2**) > *I* (Ln**3**) > *I* (Ln**1**). The results suggest that the introduction of longer fluorinated alkyl chains in the ligands, such as hfth, pfnd, are able to enhance the efficiency of energy transfer from the ligands to the central $Ln^{3+}$ ions, resulting in the improvement of the emission intensity [55,56]. The most likely reason of the differences in the emission intensity between Ln**2** and Ln**3** may be due to the differences between the thienyl substituent in the hfth ligand and the naphthyl group in the pfnd ligand [57]. The thienyl group in the hfth ligand may contribute to form a larger conjugated system, where a better energy transfer would be encouraged.

## 4. Conclusions

Nine new ternary lanthanide complexes Ln**1**, Ln**2** and Ln**3** (Ln = Er, Nd and Yb) have been synthesized based on the fluorinated-ligand tfnb, hfth and pfnd as main sensitizers, respectively, and dafone as the synergistic ligand. The DR spectra and photophysical properties of the complexes have been investigated. We have demonstrated the characteristic NIR-luminescence of the corresponding lanthanide ions upon excitation of the ligand absorption bands, mediated by the sensitizing effect of the ligands in the complexes, known as the antenna effect. The broadband emission around 1.5 μm for the Er-complexes, 1.3 μm for the Nd complex and 1 μm for the Yb-complexes could have great potential applications in optical amplifiers, laser systems and fluoroimmunoassays, respectively. The Ln**2** complexes with hfth ligand have the strongest luminescence intensities because of the most efficient intramolecular energy transfer from the hfth ligand to the central $Ln^{3+}$ ions. In addition, an indirect excitation model is proposed and antenna effect of the lanthanide complexes is discussed in detail. We found the structures of ligands have certain influences on the luminescence properties of complexes. This ligand feature is particularly important in the design of NIR-emitting lanthanide complexes and further work is in process.

## Acknowledgments

The authors are grateful to the financial aid from the National Natural Science Foundation of China (Grant No.: 20631040) and the MOST of China (Grant No.: 2006CB601103).

## Appendix A. Supplementary data

Supplementary data associated with this article can be found, in the online version, at doi:10.1016/j.jphotochem.2010.06.019.

## References

[1] G. Blasse, B.C. Grabmaier, Luminescent Materials, Springer, Berlin, Germany, 1994.
[2] R.G. Sun, Y.Z. Wang, Q.B. Zheng, H.J. Zhang, A.J. Epstein, 1.54 μm infrared photoluminescence and electroluminescence from an erbium organic compound, J. Appl. Phys. 87 (2000) 7589–7591.
[3] K. Kuriki, Y. Koike, Y. Okamoto, Plastic optical fiber lasers and amplifiers containing lanthanide complexes, Chem. Rev. 102 (2002) 2347–2356.
[4] Y. Hasegawa, T. Ohkubo, K. Sogabe, Y. Kawamura, Y. Wada, N. Nakashima, S. Yanagida, Luminescence of novel neodymium sulfonylaminate complexes in organic media, Angew. Chem. Int. Ed. 39 (2000) 357–360.
[5] J. Zhang, P.D. Badger, S.J. Geib, S. Petoud, Sensitization of near-infrared-emitting lanthanide cations in solution by tropolonate ligands, Angew. Chem. Int. Ed. 44 (2005) 2508–2512.
[6] S.I. Weissman, Intramolecular energy transfer the fluorescence of complexes of europium, J. Chem. Phys. 10 (1942) 214–217.
[7] G.E. Buono-Core, H. Li, B. Marciniak, Quenching of excited states by lanthanide ions and chelates in solution, Coord. Chem. Rev. 99 (1990) 55–87.
[8] G. Mancino, A.J. Ferguson, A. Beeby, N.J. Long, T.S. Jones, Dramatic increases in the lifetime of the $Er^{3+}$ ion in a molecular complex using a perfluorinated imidodiphosphinate sensitizing ligand, J. Am. Chem. Soc. 127 (2005) 524–525.
[9] L. Winkless, R.H.C. Tan, Y. Zheng, W.P. Gillin, Quenching of Er(III) luminescence by ligand C–H vibrations: implications for the use of erbium complexes in telecommunications, Appl. Phys. Lett. 89 (2006) 111115–111117.
[10] Y.X. Zheng, J. Lin, Y.J. Liang, Q. Lin, Y.N. Yu, Q.G. Meng, Y.H. Zhou, S.B. Wang, H.Y. Wang, H.J. Zhang, A comparative study on the electroluminescence properties of some terbium β-diketonate complexes, J. Mater. Chem. 11 (2001) 2615–2619.
[11] Y. Hasegawa, Y. Kimura, K. Murakoshi, Y. Wada, J.H. Kim, N. Nakashima, T. Yamanaka, S. Yanagida, Enhanced emission of deuterated tris(hexafluoroacetylacetonato)neodymium(III) complex in solution by suppression of radiationless transition via vibrational excitation, J. Phys. Chem. 100 (1996) 10201–10205.
[12] Y. Hasegawa, Y. Wada, S. Yanagida, Strategies for the design of luminescent lanthanide (III) complexes and their photonic applications, J. Photochem. Photobiol. C 5 (2004) 183–202.
[13] K.T. Wong, R.T. Chen, F.C. Fang, C.C. Wu, Y.T. Lin, 4,5-Diazafluoren-incorporated ter(9,9-diarylfluorene): a novel molecular doping strategy for improving the electron injection property of a highly efficient OLED blue emitter, Org. Lett. 7 (2005) 1979–1982.
[14] J.B. Yu, L. Zhou, H.J. Zhang, Y.X. Zheng, H.R. Li, R.P. Deng, Z.P. Peng, Z.F. Li, Efficient electroluminescence from new lanthanide ($Eu^{3+}$, $Sm^{3+}$) complexes, Inorg. Chem. 44 (2005) 1611–1618.
[15] L.J. Bian, H.A. Xi, X.F. Qian, J. Yin, Z.K. Zhu, Q.H. Lu, Synthesis and luminescence property of rare earth complex nanoparticles dispersed within pores of modified mesoporous silica, Mater. Res. Bull. 37 (2002) 2293–2301.
[16] H.F. Holtzclaw, J.P. Collman, Infrared absorption of metal chelate compounds of 1,3-diketone, J. Am. Chem. Soc. 79 (1957) 3318–3322.
[17] L.N. Sun, J.B. Yu, G.L. Zheng, H.J. Zhang, Q.G. Meng, C.Y. Peng, L.S. Fu, F.Y. Liu, Y.N. Yu, Syntheses, structures and near-IR luminescent studies on ternary lanthanide ($Er^{III}$,$Ho^{III}$, $Yb^{III}$,$Nd^{III}$) complexes containing 4,4,5,5,6,6,6-heptafluoro-1-(2-thienyl)hexane-1,3-dionate, Eur. J. Inorg. Chem. 19 (2006) 3962–3973.
[18] V.V. Filippov, P.P. Pershukevich, V.V. Kuznetsova, V.S. Homenko, Photoluminescence excitation properties of porous silicon with and without $Er^{3+}$–$Yb^{3+}$-containing complex, J. Lumin. 99 (2002) 185–195.
[19] W.Q. Fan, J. Feng, S.Y. Song, Y.Q. Lei, Y. Xing, R.P. Deng, S. Dang, H.J. Zhang, Erbium-complex-doped near-infrared luminescent and magnetic macroporous materials, Eur. J. Inorg. Chem. 35 (2008) 5513–5518.
[20] M. Kawa, J.M.J. Fréchet, Self-assembled lanthanide-cored dendrimer complexes: enhancement of the fluorescence properties of lanthanide cations through site-isolation and antenna effects, Chem. Mater. 10 (1998) 286–296.
[21] V. Bekiari, P. Lianos, Strongly luminescent poly(ethylene glycol)-2,2′-bipyridine lanthanide ion complexes, Adv. Mater. 10 (1998) 1455–1458.
[22] L.D. Carlos, R.A. Sá Ferreira, J.P. Rainho, V. De Zea Bermudez, Fine-tuning of the chromaticity of the emission color of organic–inorganic hybrids codoped with EuIII, TbIII, and TmIII, Adv. Funct. Mater. 12 (2002) 819–823.
[23] Y. Okamoto, Y. Ueba, N.F. Dzhanibekov, E. Banks, Rare earth metal containing polymers. 3. Characterization of ion-containing polymer structures using rare earth metal fluorescence probes, Macromolecules 14 (1981) 17–22.
[24] N. Sabbatini, A. Mecati, M. Guardigli, V. Balzani, J.M. Lehn, R. Zeissel, R. Ungaro, Lanthanide luminescence in supramolecular species, J. Lumin. 48–49 (1991) 463–468.
[25] T. Förster, Experimentelle und theoretische untersuchung des zwischemmolekularen übergangs von elektronenanregungsenergie, Z. Naturforsch. A 4 (1949) 321–327.
[26] I.B. Berlman, Energy Transfer Parameters of Aromatic Compounds, Academic Press, New York, 1973.
[27] C.Y. Peng, H.J. Zhang, J.B. Yu, Q.G. Meng, L.S. Fu, H.R. Li, L.N. Sun, X.M. Guo, Synthesis, characterization, and luminescence properties of the ternary europium complex covalently bonded to mesoporous SBA-15, j. Phys. Chem. B 109 (2005) 15278–15287.
[28] S. Dang, L.N. Sun, H.J. Zhang, X.M. Guo, Z.F. Li, J. Feng, H.D. Guo, Near-infrared luminescence from sol-gel materials doped with holmium (III) and thulium (III) complexes, J. Phys. Chem. C 112 (2008) 13240–13247.
[29] J.B. Yu, H.J. Zhang, L.S. Fu, R.P. Deng, L. Zhou, H.R. Li, F.Y. Liu, H.L. Fu, Synthesis, structure and luminescent properties of a new praseodymium(III) complex with β-diketone, Inorg. Chem. Commun. 6 (2003) 852–854.
[30] M.P.O. Wolbers, F.C.J.M. van Veggel, B.H.M. Snellink-Ruël, J.W. Hofstraat, F.A.J. Geurts, D.N. Reinhoudt, Photophysical studies of m-terphenyl-sensitized visible and near-infrared emission from organic 1:1 lanthanide ion complexes in methanol solutions, J. Chem. Soc., Perkin Trans. 2 (1998) 2141–2150.
[31] L.N. Sun, H.J. Zhang, L.S. Fu, F.Y. Liu, Q.G. Meng, C.Y. Peng, J.B. Yu, A new sol-gel material doped with an erbium complex and its potential optical-amplification application, Adv. Funct. Mater. 15 (2005) 1041–1048.
[32] S. Dang, L.N. Sun, S.Y. Song, H.J. Zhang, G.L. Zheng, Y.F. Bi, H.D. Guo, Z.Y. Guo, J. Feng, Syntheses, crystal structures and near-infrared luminescent properties of holmium (Ho) and praseodymium (Pr) ternary complexes, Inorg. Chem. Commun. 11 (2008) 531–534.
[33] J. Feng, L. Zhou, S.Y. Song, Z.F. Li, W.Q. Fan, L.N. Sun, Y.N. Yua, H.J. Zhang, A study on the near-infrared luminescent properties of xerogel materials doped with dysprosium complexes, Dalton Trans. (2009) 6593–6598.
[34] S.I. Klink, L. Grave, D.N. Reinhoudt, F.C.J.M. van Veggel, M.H.V. Werts, F.A.J. Geurts, J.W. Hofstraat, A systematic study of the photophysical processes in polydentate triphenylene-functionalized $Eu^{3+}$, $Tb^{3+}$, $Nd^{3+}$, $Yb^{3+}$, and $Er^{3+}$ complexes, J. Phys. Chem. A 104 (2000) 5457–5468.
[35] R.V. Deun, D. Moors, B.D. Fré, K. Binnemans, Near-infrared photoluminescence of lanthanide-doped liquid crystals, J. Mater. Chem. 13 (2003) 1520–1522.
[36] P. Lenaerts, K. Driesen, R. VanDeun, K. Binnemans, Covalent coupling of luminescent tris(2-thenoyltrifluoroacetonato) lanthanide (III) complexes on a Merrifield resin, Chem. Mater. 17 (2005) 2148–2154.
[37] H.J. Kim, J.E. Lee, Y.S. Kim, N.G. Park, Ligand effect on the electroluminescence mechanism in lanthanide (III) complexes, Opt. Mater. 21 (2002) 181–186.
[38] S. Comby, D. Imbert, C. Vandevyver, J.-C.G. Bünzli, A novel strategy for the design of 8-hydroxyquinolinate-based lanthanide bioprobes that emit in the near infrared range, Chem. Eur. J. 13 (2007) 936–944.
[39] P. Lenaerts, A. Storms, J. Mullens, J. D'Haen, C. Görller-Walrand, K. Binnemans, K. Driesen, Thin films of highly luminescent lanthanide complexes covalently linked to an organic–inorganic hybrid material via 2-substituted imidazo[45-f]-1,10-phenanthroline groups, Chem. Mater. 17 (2005) 5194–5201.
[40] G. Boulon, A. Collombet, A. Brenier, M.T. Cohen-Adad, A. Yoshikawa, K. Lebbou, J.H. Lee, T. Fukuda, Structural and spectroscopic characterization of nominal $Yb^{3+}$:$Ca_8La_2(PO_4)_6O_2$ oxyapatite single crystal fibers grown by the micro-pulling-down method, Adv. Funct. Mater. 11 (2001) 263–270.
[41] R.B. Thompson, Red and Near-Infrared Fluorometry, Vol.4, Plenum Press, New York, London, 1994, pp. 151–181.
[42] G.A. Casay, D.B. Shealy, G. Patonay, Near-Infrared Fluorescence Probes, vol. 4, Plenum Press, New York, London, 1994, pp. 183-222.

[43] C.V. Yang, V. Srdanov, M.R. Robonson, G.C. Bazan, A.J. Heeger, Orienting $Eu(dnm)_3$phen by tensile drawing in polyethylene: polarized $Eu^{3+}$ emission, Adv. Mater. 14 (2002) 980–983.
[44] R. Reyes, M. Cremona, E.E.S. Teotonio, H.F. Brito, O.L. Malta, Voltage color tunable OLED with (Sm,Eu)-β-diketonate complex blend, Chem. Phys. Lett. 396 (2004) 54–58.
[45] X.H. Zhu, L.H. Wang, J. Ru, W. Huang, J.F. Fang, D.G. Ma, An efficient electroluminescent (2,2′-bipyridine mono N-oxide) europium(III) β-diketonate complex, J. Mater. Chem. 14 (2004) 2732–2734.
[46] K. Binnemans, Handbook on the Physics and Chemistry of Rare Earths, vol. 35, Elsevier, Amsterdam, 2005, 225 Chapter, pp. 107–272.
[47] L.F. Yang, Z.L. Gong, D.B. Nie, Z.Q. Bian, M. Guan, C.H. Huang, H.J. Lee, W.P. Baik, Promoting near-infrared emission of neodymium complexes by tuning the singlet and triplet energy levels of β-diketonates, New J. Chem. 30 (2006) 791–796.
[48] D.L. Dexter, A theory of sensitized luminescence in solids, J. Chem. Phys. 21 (1953) 836–850.
[49] L.N. Sun, J.B. Yu, H.J. Zhang, Q.G. Meng, E. Ma, C.Y. Peng, K.Y. Yang, Near-infrared luminescent mesoporous materials covalently bonded with ternary lanthanide [Er(III), Nd(III), Yb(III), Sm(III), Pr(III)] complexes, Micropor. Mesopor. Mater. 98 (2007) 156–165.
[50] G.A. Crosby, R.E. Whan, R.M. Alire, Intramolecular energy transfer in rare earth chelates. role of the triplet state, J. Chem. Phys. 34 (1961) 743–748.
[51] W. Sager, N. Filipescu, F.A. Serafin, Substituent effects on intramolecular energy transfer. I. Absorption and phosphorescence spectra of rare earth β-diketone chelates, J. Phys. Chem. 69 (1965) 1092–1100.
[52] F. Quochi, R. Orrù, F. Cordella, A. Mura, G. Bongiovanni, F. Artizzu, P. Deplano, M.L. Mercuri, L. Pilia, A. Serpe, Near infrared light emission quenching in organolanthanide complexes, J. Appl. Phys. 99 (2006) 053520–053524.
[53] R. Van Deun, P. Fias, P. Nockemann, K. Van Hecke, L. Van Meervelt, K. Binnemans, Rare-earth nitroquinolinates: visible-light-sensitizable near-infrared emitters in aqueous solution, Eur. J. Inorg. Chem. 20 (2007) 302–305.
[54] L. Shen, M. Shi, F.Y. Li, D.Q. Zhang, X.H. Li, E.X. Shi, T. Yi, Y.K. Du, C.H. Huang, Polyaryl ether dendrimer with a 4-phenylacetyl-5-pyrazolone-based terbium(III) complex as core: synthesis and photopysical properties, Inorg. Chem. 45 (2006) 6188–6197.
[55] M. Latva, H. Takalo, K. Simberg, J. Kankare, Enhanced EuIII ion luminescence and efficient energy transfer between lanthanide chelates within the polymeric structure in aqueous solutions, J. Chem. Soc. Perkin Trans. 2 (1995) 995–999.
[56] M. Iwamuro, Y. Wada, T. Kitamura, N. Nakashim, S. Yanagida, Photosensitized luminescence of novel β-diketonato Nd(III) complexes in solution, Phys. Chem. Chem. Phys. 2 (2000) 2291–2296.
[57] L.H. Wang, W. Wang, W.G. Zhang, E.T. Kang, W. Huang, Synthesis and luminescence properties of novel Eu-containing copolymers consisting of Eu(III)-acrylate-β-diketonate complex monomers and methyl methacrylate, Chem. Mater. 12 (2000) 2212–2218.